Scientific Publications

World Journal of Civil Engineering and Architecture, 2026, 4, 6906
www.scipublications.com/journal/wjcea
DOI: 10.31586/wjcea.2026.6906

Article

Early-age chemical and autogenous shrinkage of cement pastes containing palm oil fuel ash at different water-to-binder ratios

Tchemou Gilbert [1], Tubuo Fabian Mawen [1,*], Jenny Alban Otsobo Ambassa [2], Nkwenti Flavious Tanue [3], Nkemaja Dydimus Efeze [4]

[1] Post Graduate Training Unit for Engineering Sciences, University of Douala, Douala, Cameroon

[2] Department of Fundamental and Cross-Cutting Sciences, National Advanced School of Public Works, P.O. Box 510, Yaoundé, Cameroon

[3] National Higher Polytechnic Institute, University of Bamenda, Bamenda, Cameroon

[4] Department of Social Economy and Family Management, Higher Technical Teacher Training College (HTTTC), The University of Bamenda, P.O. Box 39, Bambili, North-West Region, Cameroon.

*Correspondence: Tubuo Fabian Mawen

Abstract: This study investigates the effects of palm oil fuel ash (POFA) incorporation and water-to-binder ratio on the chemical shrinkage (CS) and autogenous shrinkage (AS) of cement pastes. Cement is partially replaced with ground POFA at levels of 0, 10, 20 and 30%, while the water-to-binder ratio (w/b) varies between 0.3, 0.4 and 0.5. Both shrinkage mechanisms were measured during the first 24 h using hydrostatic weighing based on Archimedes' principle. CS was determined on paste specimens immersed in water in open crystallisation dishes, whereas AS was measured volumetrically on specimens sealed in latex membranes. The results show that the w/b ratio has only a minor influence on 24-h CS, which decreases by approximately 8% on average as the ratio increases from 0.3 to 0.5. In contrast, AS is strongly influenced by the w/b ratio, with the 24-h value for the control paste decreasing by approximately 23%, from 35.8×10^{-3} to 27.5×10^{-3} cm³/g, over the same range. A 10% POFA replacement produces the lowest CS at all three w/b ratios, with reductions of 8.1–10.7% relative to the corresponding control pastes. However, replacement levels of 20 and 30% result in CS values comparable to or up to 7.5% higher than those of the control, together with a faster increase during the 15–24 h interval. The influence of POFA on AS remains comparatively small, with variations ranging from −8.6% to +3.4%. The 24-h AS/CS ratio exceeds unity in several mixtures, particularly at lower w/b ratios, pointing to limitations in the comparability of the two measurement procedures. Overall, the findings indicate that 10% POFA reduces chemical shrinkage without substantially increasing autogenous shrinkage during the first 24 h.

Keywords: Palm oil fuel ash; Chemical shrinkage; Autogenous shrinkage; Early age; Water-to-binder ratio; Hydrostatic weighing

How to cite this paper:
Gilbert, T., Mawen, T. F., Ambassa, J. A. O., Tanue, N. F., & Efeze, N. D. (2026). Early-age chemical and autogenous shrinkage of cement pastes containing palm oil fuel ash at different water-to-binder ratios. *World Journal of Civil Engineering and Architecture*, *4*(1), 41-59.
DOI: 10.31586/wjcea.2026.6906

Received: October 2, 2026
Revised: November 6, 2026
Accepted: November 12, 2026
Published: November 13, 2026

Copyright: © 2026 by the authors. Submitted for possible open access publication under the terms and conditions of the Creative Commons Attribution (CC BY) license (http://creativecommons.org/licenses/by/4.0/).

1. Introduction

Concrete is the most widely used manufactured material in the world [1] and plays a central role in civil engineering. Continuous developments in concrete technology have led to the production of high-strength and high-performance concretes, often characterised by low water-to-cement ratios. Although these materials offer improved mechanical performance, their low water content can promote early-age volume changes and increase their susceptibility to cracking [2]. Early-age cracking is a major concern because it can compromise the integrity and long-term durability of concrete structures. Consequently, understanding the behaviour of cementitious materials during the first

hours after mixing, particularly at the paste scale, remains an important research challenge.

In parallel, the increasing generation of agricultural and industrial waste has raised environmental concerns related to its disposal and the consumption of natural resources. The incorporation of suitable waste-derived materials as supplementary cementitious materials (SCMs) offers an opportunity to reduce cement consumption while promoting waste valorisation. Palm oil fuel ash (POFA), a residue generated by the combustion of palm fibres, shells and empty fruit bunches in boilers at palm oil processing mills, has attracted attention because of its potential pozzolanic properties [3,4]. Its use in cement-based materials could therefore contribute to the recovery of an agro-industrial by-product while reducing the demand for conventional cement constituents. However, the suitability of POFA as a cement replacement depends on its physical and chemical characteristics, processing conditions and effects on the properties of fresh and hardened cementitious materials.

Previous investigations into POFA-based cementitious materials have mainly focused on mechanical performance and durability. Regarding compressive strength, Muthusamy and Zamri [6] identified 20% POFA as an effective cement replacement level for improving 28-day strength, whereas Islam et al. [7] reported an optimum replacement level of 10%. Zeyad et al. [8] demonstrated that ultrafine POFA can contribute to the production of high-strength concrete, with 28-day compressive strengths exceeding 90 MPa. Tangchirapat et al. [9] also showed that the performance of POFA depends strongly on its particle size. Beyond mechanical properties, previous studies have reported that POFA can reduce the workability of fresh concrete [7,10,11] and delay initial and final setting times [7,9,12]. Its influence on durability has also been investigated in relation to chloride penetration [13], sulfate attack [9,14], heat of hydration [15], water permeability [16], elevated-temperature performance [17] and thermal properties [18-22]. These studies demonstrate the potential of POFA in cement-based materials, but they also indicate that its effects depend on the material characteristics and the properties being evaluated.

Despite these investigations, the influence of POFA on the early-age volume stability of cementitious materials remains insufficiently understood. In particular, limited attention has been given to chemical shrinkage (CS) and autogenous shrinkage (AS) during the first hours following mixing. Safiuddin et al. [3] highlighted the limited number of studies addressing the influence of POFA on plastic shrinkage, while previous investigations have mainly considered drying shrinkage in hardened concrete [11]. Chemical and autogenous shrinkage are nevertheless important early-age phenomena because they are associated with cement hydration, internal volume changes and the development of self-induced stresses that may contribute to early-age cracking [2,23]. Furthermore, POFA may influence these processes through clinker dilution, changes in water demand and delayed setting [7,9,12]. Its effect on chemical and autogenous shrinkage therefore cannot be reliably inferred from compressive strength, workability or setting-time results alone. This raises two related scientific questions: how do POFA replacement level and water-to-binder ratio affect chemical and autogenous shrinkage during the first 24 h, and how do the measured responses of these two shrinkage mechanisms relate to each other?

Addressing these questions requires the simultaneous investigation of chemical and autogenous shrinkage under different mixture conditions. Although previous studies have examined several properties of POFA-based cementitious materials, the combined assessment of these two early-age deformation mechanisms across different POFA replacement levels and water-to-binder ratios remains limited. The contribution of the present study lies in examining both phenomena within the same experimental programme, using a common gravimetric measurement principle based on hydrostatic weighing but different specimen configurations. This approach makes it possible to compare their responses to changes in binder composition and water availability and to

examine the relationship between the measured deformations. The study therefore investigates cement pastes in which 0, 10, 20 and 30% of the cement is replaced by ground POFA, at water-to-binder ratios (w/b) of 0.3, 0.4 and 0.5, over the first 24 h following water–binder contact. Specifically, its objectives are to (i) quantify the influence of the w/b ratio on chemical and autogenous shrinkage, (ii) assess the influence of POFA replacement level on both deformation mechanisms, and (iii) examine the relationship between chemical and autogenous shrinkage.

The remainder of this paper is organised as follows. Section 2 presents the theoretical background of chemical and autogenous shrinkage and reviews the characteristics of POFA. Section 3 describes the materials, mixture proportions and experimental procedures used to measure both shrinkage mechanisms. Section 4 presents and discusses the experimental results, focusing on the development of chemical and autogenous shrinkage, the effects of water-to-binder ratio and POFA replacement level, and the relationship between the two deformations. Finally, Section 5 presents the main conclusions and directions for further research.

2. Background

2.1. Chemical shrinkage

As first observed by Le Chatelier, the hydration of cement leads to a reduction in the absolute volume of the reacting system, as the hydration products generally occupy a smaller volume than the initial cement and water [23,24]. This phenomenon is known as chemical shrinkage (CS). Since it is directly related to the progress of cement hydration, CS is commonly used as an indicator of the extent of hydration [25,26]. The hydration of the main clinker phases, particularly tricalcium silicate (C_3S), dicalcium silicate (C_2S), tricalcium aluminate (C_3A), and tetracalcium aluminoferrite (C_4AF), produces various hydration products, including calcium silicate hydrate (C–S–H), calcium hydroxide, and aluminate- and ferrite-containing hydrates [27]. In principle, chemical shrinkage can be calculated from the difference between the initial volume of the reacting constituents and the volume of the hydration products formed [23]. The absolute chemical shrinkage volume is expressed as:

$$\Delta V_{CS} = V_c + V_w - V_{hy} \quad (1)$$

The relative chemical shrinkage, expressed as a percentage of the initial volume of the cement–water system, is then given by:

$$CS(\%) = \frac{\Delta V_{CS}}{V_{ci}+V_{wi}} \times 100 \quad (2)$$

where V_{ci} and V_{wi} represent the initial volumes of cement and water before mixing, respectively; V_c and V_w denote the volumes of cement and water that have reacted, respectively; and V_{hy} is the total volume of the hydration products formed. In practice, determining the individual volumes of the reacting phases and hydration products requires sophisticated experimental techniques. Consequently, chemical shrinkage is generally measured directly using dedicated experimental methods.

2.2. Autogenous shrinkage

Autogenous shrinkage (AS) is defined as the macroscopic volume change of a cementitious material occurring under sealed conditions, without moisture exchange with the surrounding environment, at constant temperature and in the absence of external loading. The term was introduced by Lynam in 1934 [23]. Autogenous shrinkage is closely related to chemical shrinkage (CS), as both phenomena originate from cement hydration. Before setting, while the cement paste remains sufficiently fluid, chemical shrinkage can

be accommodated by the free movement of the paste, and the two volume changes may be approximately equivalent. However, once a load-bearing solid skeleton develops, the paste can no longer contract freely. Consequently, an increasing proportion of the chemical shrinkage is accommodated by the formation of internal voids rather than by an equivalent external volume reduction [23,24].

As hydration progresses, the consumption of water leads to the development of empty or partially water-filled capillary pores. The formation of water–air menisci within these pores generates capillary pressure. This pressure increases as the menisci develop in progressively finer pores, producing compressive stresses within the solid skeleton and contributing to autogenous shrinkage through self-desiccation [24,28,29]. This phenomenon is particularly significant in cementitious systems with a low water-to-cement ratio (w/c). Below a w/c ratio of approximately 0.40, the amount of available water may become insufficient to sustain complete hydration, thereby promoting self-desiccation [2]. Since only a fraction of the chemical shrinkage is converted into external deformation after the formation of the solid skeleton, autogenous shrinkage is generally expected to remain lower than chemical shrinkage from this stage onwards [23].

2.3. Palm oil fuel ash

Palm oil processing generates substantial quantities of solid residues, mainly empty fruit bunches, palm shells and palm fibres, which account for approximately 70–75% of the processed fruit mass. These residues are commonly used as fuel in boilers at palm oil mills. Combustion temperatures can reach approximately 1000 °C [30], while the resulting ash represents about 5% of the burnt waste [31,32]. The annual production of palm oil fuel ash (POFA) is estimated at more than 3 million tonnes in Malaysia [30] and over 100,000 tonnes in Thailand [33].

The physical and chemical properties of POFA depend strongly on the combustion conditions and subsequent processing methods. Incomplete combustion, particularly at relatively low temperatures, generally results in a high residual carbon content and produces dark grey to black ash. Conversely, higher combustion temperatures are often associated with lighter-coloured ash and improved material characteristics [34,35]. In its as-received condition, POFA generally consists of coarse and porous particles. It is therefore commonly subjected to grinding, using equipment such as modified Los Angeles abrasion machines or ball mills, to improve its fineness and modify its physical characteristics [33, 35, 36]. The specific gravity of unground POFA typically ranges from 1.78 to 1.97, approximately 40% lower than that of Portland cement [37]. Following grinding, this value can increase to between 2.22 and 2.78 [9,38]. Grinding also reduces the median particle size from approximately 54–183 μm to 7–10 μm [38] and modifies the particle morphology, transforming large, porous and approximately spherical particles into smaller, crushed and angular particles with characteristics similar to those of cement particles [16]. The preparation procedures reported in the literature vary considerably, ranging from simple oven-drying and sieving [30,33] to more elaborate treatments involving successive grinding and re-burning stages to reduce the unburnt carbon content and produce ultrafine ash [8].

From a chemical perspective, silica (SiO_2) is generally the predominant oxide in POFA, with reported contents ranging from 44% to 66%. Aluminium oxide (Al_2O_3) and iron oxide (Fe_2O_3) are also present, while the loss on ignition (LOI) varies widely, from 0.1% to 21.5% [3]. The classification of POFA according to ASTM C618 [39] is not consistent across the literature. Depending on the chemical composition of the ash investigated, some studies have classified it as Class N [33,38], others as Class F based on its low CaO content [40], while Class C has also been reported [41]. These differences highlight the considerable variability of POFA and the importance of characterising each ash source before assessing its suitability for use as a supplementary cementitious material.

3. Materials and methods

3.1. Cement

A Portland composite cement (CEM II 42.5 R; CPA-CEM II), manufactured by Cimencam and complying with the Cameroonian standard NC 234-2005-06, was used in this study. This cement was selected because of its widespread use in Cameroon. Two 50-kg bags were purchased from a local retailer immediately after delivery from the manufacturing plant. Upon receipt, the cement was divided into approximately 1-kg portions, vacuum-sealed in plastic bags, and stored in a dry laboratory container until use to minimise exposure to atmospheric moisture and prevent premature hydration.

Previous experimental investigations have characterised CEM II 42.5 R cement manufactured by CIMENCAM in Cameroon. For instance, [44] reported a Blaine specific surface area of 3418 cm^2/g (341.8 m^2/kg) and a normal consistency of 32% for the CIMENCAM cement investigated. These findings provide a useful reference for the physical characteristics of commercially available cement in Cameroon. However, they are not measurements of the cement batch used in the present study. Accordingly, the mineralogical composition and physical properties reported in the manufacturer's technical data sheet are presented in Tables 1 and 2, respectively. The experimentally determined physical properties of the ground palm oil fuel ash (POFA) are also included in Table 2 for comparison.

Table 1. Mineralogical composition of the cement (manufacturer's technical data sheet, Cimencam).

Phase	Chemical formula	Notation	Content (wt.%)
Tricalcium silicate	$3CaO{\cdot}SiO_2$	C_3S	55–70
Dicalcium silicate	$2CaO{\cdot}SiO_2$	C_2S	10–25
Tricalcium aluminate	$3CaO{\cdot}Al_2O_3$	C_3A	5–13
Tetracalcium aluminoferrite	$4CaO{\cdot}Al_2O_3{\cdot}Fe_2O_3$	C_4AF	1–15
Gypsum	$CaSO_4{\cdot}2H_2O$	$C\bar{S}H_2$	≤ 3.5

Table 2. Physical properties of the cement (manufacturer's technical data sheet, Cimencam) and of the ground POFA (measured).

Property	Cement	POFA
Absolute density (g/cm^3)	2.8–3.2	—
Specific gravity	—	2.1
Bulk density (g/cm^3)	0.9–1.2	—
Blaine specific surface (m^2/kg)	—	506
Particles < 5 μm (%)	20–30	—
Initial setting time (min)	60–90	—
Solubility in water at 20 °C (g/L)	1.5	—

3.2. Palm oil fuel ash

Palm oil fuel ash (POFA) was collected from a palm oil processing mill located in Souza, Moungo Division, Cameroon, where palm fibres, shells, and empty fruit bunches

are used as boiler fuel. The collected ash was oven-dried at 105 °C for 24 h to remove residual moisture and subsequently sieved through an 80 μm mesh to eliminate coarse particles and foreign impurities. The sieved material was then mechanically ground for 6 h using a Deval attrition machine operating at a rotational speed of 100 ± 5 rpm. Following grinding, the fraction passing through a 45 μm sieve, representing approximately 60% of the ground ash, was retained for the experimental programme (Figure 1). The processed POFA exhibited a specific gravity of 2.1 and a Blaine specific surface area of 506 m²/kg, as reported in Table 2.

Previous studies have demonstrated that the chemical composition and physical characteristics of POFA depend strongly on the nature of the biomass, combustion conditions, and subsequent processing. [45] identified silica as a major constituent of thermally treated POFA through X-ray fluorescence (XRF) and X-ray diffraction (XRD) analyses. Similarly, [46] reported a silica content of 63.4% and a loss on ignition of 6.0% for POFA processed for use as a cementitious binder. More recently, experimental investigations have reported silica contents of approximately 62.8% in POFA [47], further highlighting its potential as a supplementary cementitious material. However, these values are specific to the materials and processing conditions investigated in the respective studies and cannot be assumed to represent the chemical composition of the POFA collected in Souza.



Figure 1. Preparation of the POFA: (a) ash as collected from the mill; (b) grinding in the Deval machine; (c) sieve stack; (d) ground and sieved POFA.

Twelve cement pastes were prepared using four POFA replacement levels (0, 10, 20, and 30% by mass of the total binder) and three water-to-binder ratios (w/b = 0.3, 0.4, and 0.5), resulting in twelve different mixtures (Table 3). The binder consisted of Portland composite cement and POFA, with POFA partially replacing cement by mass. Accordingly, the w/b ratio was calculated as the mass of mixing water divided by the total mass of binder (cement + POFA).

Demineralised water was used for all mixtures. Paste preparation followed a controlled mixing sequence. First, the cement and POFA were blended at low speed for 1 min, while approximately three-quarters of the required mixing water was gradually added. Mixing was then continued at high speed for 1 min. The mixer was subsequently stopped for 1 min to allow the walls of the mixing bowl to be scraped and any adhering material to be incorporated into the paste. The remaining water was then added gradually during 1 min of low-speed mixing, followed by a final 1 min of high-speed mixing to ensure adequate homogenisation.

The total mixing time, measured from the first contact between water and binder, was 5 min. The same mixing procedure was applied to all twelve mixtures to maintain

consistent preparation conditions and minimise variations associated with the mixing process.

Table 3. Mixture proportions per 100 g of binder.

Mixture	w/b	POFA (%)	Cement (g)	POFA (g)	Water (g)
P0-0.3	0.3	0	100	0	30
P10-0.3	0.3	10	90	10	30
P20-0.3	0.3	20	80	20	30
P30-0.3	0.3	30	70	30	30
P0-0.4	0.4	0	100	0	40
P10-0.4	0.4	10	90	10	40
P20-0.4	0.4	20	80	20	40
P30-0.4	0.4	30	70	30	40
P0-0.5	0.5	0	100	0	50
P10-0.5	0.5	10	90	10	50
P20-0.5	0.5	20	80	20	50
P30-0.5	0.5	30	70	30	50

3.4. Measurement of chemical shrinkage

Chemical shrinkage was measured gravimetrically by monitoring changes in the buoyancy of paste specimens immersed in water, following the procedure described in ASTM C1608 [42]. Fresh cement paste (50–80 g) was placed in a cylindrical crystallisation dish with a diameter of 70 mm and a height of 50 mm. The dish was then vibrated until the paste formed a relatively uniform layer with a thickness of 15–24 mm, depending on the mass of paste used (Figure 2).

As no vacuum chamber was available, complete removal of entrapped air from the fresh paste could not be ensured. To minimise the presence of air bubbles, the water used in the measurement was first de-aired by boiling for a few minutes. Approximately 10 g of this water was then gently applied to the paste surface using a syringe until a continuous water film formed. Distilled water was subsequently added dropwise until the paste surface was completely covered, after which the dish was filled almost to its upper edge.

The crystallisation dish was placed on a stainless-steel mesh platform suspended by a monofilament line from a hook connected to an electronic balance equipped with internal memory for automatic data acquisition. The balance was positioned on a massive table to minimise external vibrations. The dish was carefully lowered into a plastic container holding approximately 30 L of distilled water. This container was immersed in a temperature-controlled water bath maintained at 28 ± 0.5 °C, with continuous water circulation. The bath contained approximately 25 L of water and was covered with an acrylic lid to limit evaporation. The distilled water used in the experiments was produced in the laboratory by boiling tap water and condensing the resulting vapour.

Mass measurements under submerged conditions began approximately 30 min after the initial contact between water and binder, which was defined as the reference time (t = 0). The submerged mass was subsequently recorded automatically at 3-h intervals.



(a) (b)

Figure 2. (a) Paste specimen for the chemical shrinkage test; (b) hydrostatic weighing set-up with the balance above the immersion bath.

3.5. Measurement of autogenous shrinkage

Autogenous shrinkage was measured volumetrically by monitoring changes in the submerged mass of fresh cement paste specimens sealed in elastic membranes, following the method described in [43]. Thin latex membranes (Plan type, Guilin Latex, China) were used because of their availability and their watertight properties, which minimise the risk of water penetration during testing. Before filling, the lubricant on the external surface of each membrane was carefully removed using a soft paper towel.

Approximately 100–150 g of fresh paste was introduced into each membrane. The membrane was then tightly closed with a knot, taking care to minimise the entrapment of air. The excess membrane material was trimmed, and a monofilament line (0.12 mm in diameter and approximately 400 mm long) was attached to the specimen using a plastic strap. The other end of the line was connected to a stainless-steel hook suspended beneath the electronic balance.

Each sealed specimen was gently immersed in a plastic container filled with distilled water and placed in a temperature-controlled water bath. Air bubbles adhering to the upper surface of the membrane were carefully removed after immersion. The submerged mass was automatically recorded at 60-min intervals, starting approximately 30 min after the first contact between water and binder. The first reading taken after immersion was discarded because the specimen was still undergoing oscillations. Any water droplets adhering to the suspension line fell into the bath within the first minute and were therefore not considered to affect subsequent measurements.

To assess the watertightness of the membranes, the mass of each specimen in air was measured before and after the test. Any difference between these measurements was used to evaluate possible water penetration through the membrane.

3.6. Data analysis

Both chemical shrinkage (CS) and autogenous shrinkage (AS) were determined from changes in the apparent submerged mass of the specimens, based on Archimedes' principle. The reduction in specimen volume was calculated from the increase in apparent submerged mass relative to the initial reference measurement. The shrinkage values were then normalised by the mass of binder contained in each specimen. Accordingly, CS and AS were calculated using:

$$CS(t), AS(t) = \frac{|m_{W,0} - m_W(t)| \cdot (1 + w/b)}{m_p \cdot \rho} \quad (3)$$

where $m_W(t)$ is the apparent submerged mass at time t, $m_{W,0}$ is the apparent submerged mass at the initial reference measurement, m_p is the initial mass of fresh paste, w/b is the water-to-binder ratio, and ρ is the density of the immersion liquid. The shrinkage values are expressed in cm^3/g of binder when masses are expressed in grams and density in g/cm^3.

To compare the shrinkage kinetics, the average shrinkage rate over each selected time interval was calculated as:

$$R = \frac{(S(t_2) - S(t_1))}{t_2 - t_1} \quad (4)$$

where S represents either CS or AS, and t_1 and t_2 are the initial and final times of the considered interval, respectively. The intervals considered were 0–9 h, 9–15 h and 15–24 h. The relative change in shrinkage associated with POFA incorporation was calculated with respect to the corresponding control paste (0% POFA) at the same water-to-binder ratio:

$$\Delta S(\%) = \frac{S_{POFA} - S_{control}}{S_{control}} \times 100 \quad (5)$$

where S_{POFA} and $S_{control}$ represent the shrinkage values of the POFA-containing paste and the corresponding reference paste, respectively. Negative values indicate a reduction in shrinkage, whereas positive values indicate an increase relative to the control.

A total of 24 tests were performed, corresponding to one chemical shrinkage test and one autogenous shrinkage test for each of the 12 mixtures. Since no replicate measurements were performed, statistical tests could not be applied. Consequently, the differences observed between mixtures are interpreted as experimental trends rather than statistically significant effects.

4. Results and discussion

4.1. Development of chemical shrinkage

The evolution of chemical shrinkage (CS) in the cement pastes during the first 24 h is presented in Figure 3. The corresponding 24-h values are summarised in Table 4, while the complete experimental data are provided in Appendix A. All mixtures exhibit a continuous increase in CS throughout the monitoring period, indicating that hydration-related volume contraction was still progressing at the end of the test. The 24-h CS values range from 26.7 to 34.6 × 10^{-3} cm^3/g of binder, depending on the mixture composition. Although the overall evolution follows a similar increasing trend, differences in the final values indicate that the early-age chemical shrinkage is influenced by the water-to-binder ratio and the level of POFA replacement.

Chemical shrinkage is directly associated with the consumption of anhydrous cement phases and the formation of hydration products [25,26]. Consequently, its continuous increase reflects the ongoing hydration of the cementitious system during the first 24 h. The influence of the individual mixture parameters on the measured CS is examined in the following sections.

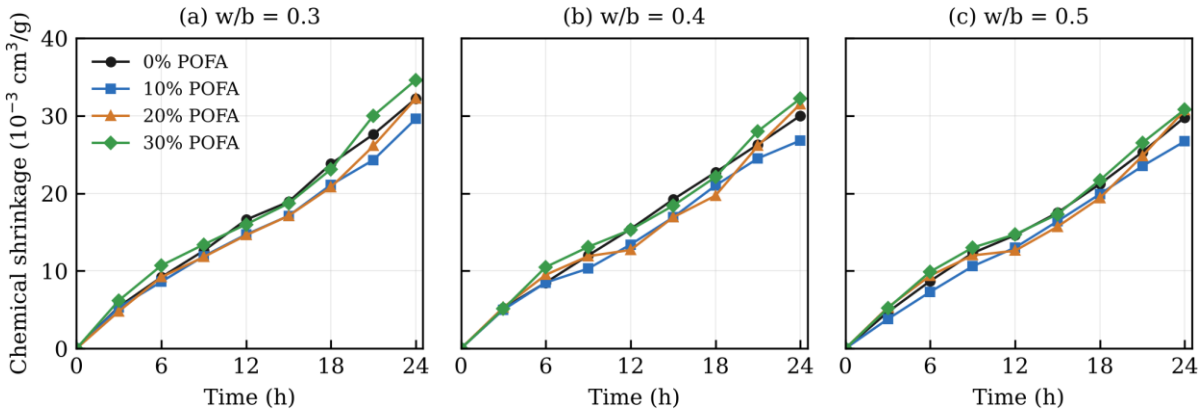


Figure 3. Chemical shrinkage of the pastes with 0–30% POFA during the first 24 h at w/b of (a) 0.3, (b) 0.4 and (c) 0.5.

4.2. Effect of the water-to-binder ratio on chemical shrinkage

The influence of the water-to-binder ratio on chemical shrinkage (CS) is illustrated in Figure 5a for the control paste. The three curves follow a similar evolution and remain relatively close throughout the 24-h monitoring period, indicating that the w/b ratio has a limited influence on CS under the conditions investigated. At 24 h, the measured CS decreases slightly from 32.2 × 10^{-3} cm³/g of binder at w/b = 0.3 to approximately 30.0 × 10^{-3} cm³/g at w/b = 0.4 and 0.5. Overall, increasing the w/b ratio produces only a modest reduction in chemical shrinkage.

This limited variation suggests that the amount of water initially available does not substantially alter the extent of chemical shrinkage during the first 24 h. The slightly higher value observed at w/b = 0.3 may be associated with differences in early hydration kinetics. This observation is consistent with Mounanga [26], who reported faster early hydration in cement pastes with lower w/c ratios. However, the present results do not allow this explanation to be established conclusively.

4.3. Effect of POFA on chemical shrinkage

The influence of POFA replacement on chemical shrinkage is shown in Figure 6a, with the corresponding 24-h values reported in Table 4. A non-monotonic response is observed at all three water-to-binder ratios. The incorporation of 10% POFA consistently produces the lowest CS, reducing the 24-h values by approximately 8–11% compared with the corresponding control pastes. However, increasing the POFA content to 20% and 30% does not result in further reductions. Instead, CS becomes comparable to or higher than that of the control, with increases reaching approximately 7.5% at the highest replacement level.

The reduction observed at 10% POFA may partly be attributed to the dilution of the cement, which decreases the amount of clinker available for hydration per unit mass of binder. The contribution of the pozzolanic reaction is also expected to be limited during the first 24 h [3,4]. However, the higher CS values recorded at 20% and 30% POFA indicate that dilution alone cannot account for the observed behaviour.

The higher CS at these replacement levels may be associated with changes in the early hydration process, potentially influenced by the delayed setting of POFA-containing pastes reported in previous studies [7,9,12]. Nevertheless, this interpretation remains tentative because hydration kinetics were not directly monitored in the present study. Moreover, the possible influence of water uptake by the porous POFA particles on the gravimetric measurements cannot be excluded. Further investigations involving

isothermal calorimetry and thermogravimetric analysis would be necessary to clarify the mechanisms responsible for the observed response.

Table 4. Chemical (CS) and autogenous (AS) shrinkage at 24 h, change relative to the control at the same w/b, and AS/CS ratio.

w/b	POFA (%)	CS_{24} (10^{-3} cm^3/g)	ΔCS (%)	AS_{24} (10^{-3} cm^3/g)	ΔAS (%)	AS/CS
0.3	0	32.2	—	35.8	—	1.11
0.3	10	29.6	−8.1	35.1	−2.0	1.19
0.3	20	32.2	0.0	37.0	+3.4	1.15
0.3	30	34.6	+7.5	34.4	−3.9	0.99
0.4	0	30.0	—	32.4	—	1.08
0.4	10	26.8	−10.7	30.7	−5.2	1.15
0.4	20	31.5	+5.0	31.6	−2.5	1.00
0.4	30	32.2	+7.3	29.6	−8.6	0.92
0.5	0	29.8	—	27.5	—	0.92
0.5	10	26.7	−10.4	26.4	−4.0	0.99
0.5	20	30.7	+3.0	27.4	−0.4	0.89
0.5	30	30.8	+3.4	27.4	−0.4	0.89

ΔCS and ΔAS: change relative to the 0% POFA paste at the same w/b; negative values indicate lower shrinkage than the control.

Table 5. Average shrinkage rates over three-time intervals (10^{-3} $cm^3/(g{\cdot}h)$).

w/b	POFA (%)	CS 0–9 h	CS 9–15 h	CS 15–24 h	AS 0–9 h	AS 9–15 h	AS 15–24 h
0.3	0	1.40	1.05	1.48	1.60	1.32	1.50
0.3	10	1.32	0.87	1.39	1.36	1.47	1.57
0.3	20	1.31	0.88	1.68	1.74	1.47	1.39
0.3	30	1.49	0.88	1.77	1.31	1.33	1.62
0.4	0	1.33	1.20	1.20	1.38	1.45	1.26
0.4	10	1.14	1.10	1.10	1.26	1.43	1.20
0.4	20	1.32	0.83	1.62	1.53	1.25	1.14
0.4	30	1.46	0.88	1.53	1.22	0.95	1.43
0.5	0	1.37	0.87	1.37	1.02	1.38	1.11
0.5	10	1.18	0.97	1.14	1.09	1.43	0.89
0.5	20	1.33	0.62	1.67	1.18	1.25	1.03
0.5	30	1.44	0.72	1.50	1.03	1.30	1.14

4.4. Development of autogenous shrinkage

Figure 4 illustrates the evolution of autogenous shrinkage (AS) in the cement pastes during the first 24 h. All mixtures exhibit a continuous and approximately linear increase in AS throughout the monitoring period. Unlike chemical shrinkage, no pronounced changes in the slope of the curves are observed. At 24 h, the measured AS values range from 26.4 to 37.0 × 10^{-3} cm^3/g of binder, depending on the mixture composition (Table 4).

This overall evolution indicates that autogenous deformation progressively develops during the early hydration of the cement pastes.

Autogenous shrinkage is associated with hydration-induced volume changes and the development of self-desiccation as the cement paste progressively forms a solid skeleton [24,28]. The resulting deformation is also influenced by the evolving mechanical properties of the paste. The continuous increase observed in Figure 4 therefore reflects the progressive development of autogenous shrinkage during the first 24 h.

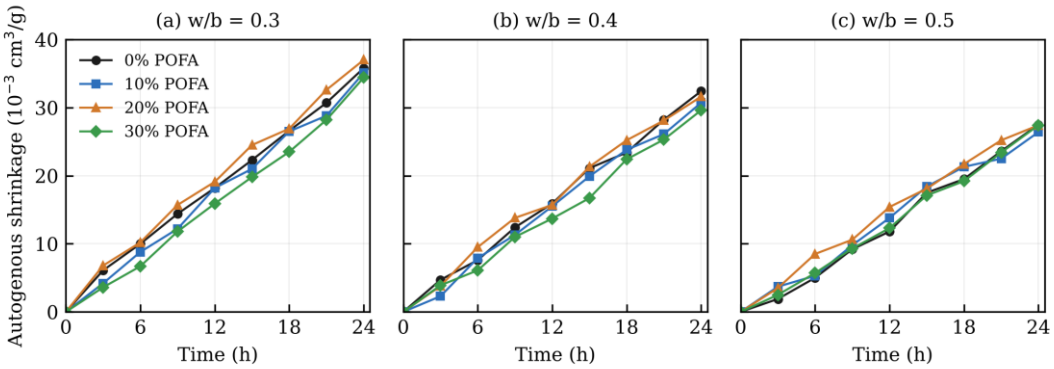


Figure 4. Autogenous shrinkage of the pastes with 0–30% POFA during the first 24 h at w/b of (a) 0.3, (b) 0.4 and (c) 0.5.

4.5. Effect of the water-to-binder ratio on autogenous shrinkage

The influence of the water-to-binder ratio on autogenous shrinkage (AS) is illustrated in Figure 5b. Unlike chemical shrinkage, AS is strongly affected by the initial water content. The curves become progressively more separated as the w/b ratio increases, with lower AS values consistently observed at higher w/b ratios. For the control paste, the 24-h AS decreases from 35.8 × 10^{-3} cm^3/g of binder at w/b = 0.3 to 27.5 × 10^{-3} cm^3/g at w/b = 0.5, corresponding to a reduction of approximately 23%.

This behaviour is consistent with the self-desiccation mechanism, which is more pronounced in cement pastes with low water-to-binder ratios [2,24]. At lower w/b ratios, the limited availability of water promotes the development of capillary menisci and generates higher capillary stresses within the pore structure. These stresses induce contraction of the developing solid skeleton, resulting in greater autogenous shrinkage. The observed dependence of AS on w/b is also consistent with previous investigations of Portland cement pastes [23,28].

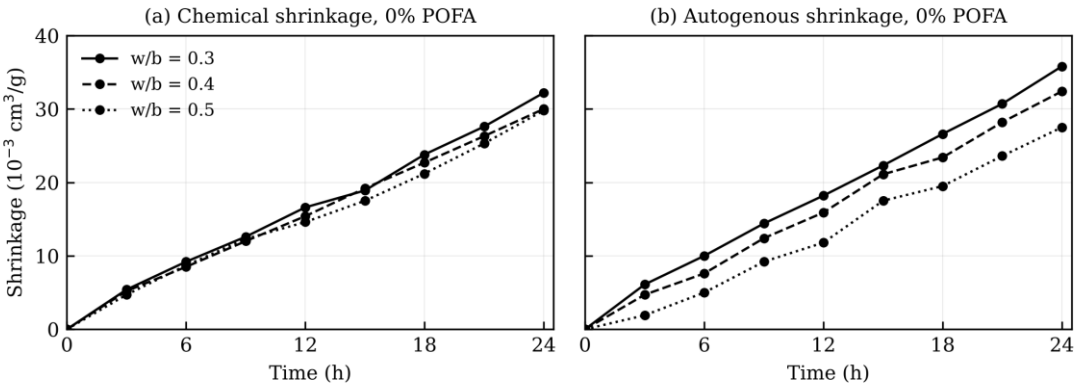


Figure 5. Effect of the w/b on (a) chemical shrinkage and (b) autogenous shrinkage of the control paste (0% POFA).

4.6. Effect of POFA on autogenous shrinkage

Figure 6b shows that POFA incorporation has a limited influence on the 24-h autogenous shrinkage (AS). The values obtained for the POFA-containing pastes remain relatively close to those of the corresponding control mixtures, with variations ranging from −8.6% to +3.4%. Most mixtures exhibit slightly lower AS than their respective controls, although no consistent reduction with increasing POFA content is observed.

These results suggest that replacing up to 30% of the cement with POFA does not substantially increase autogenous shrinkage during the first 24 h. However, since only one measurement was performed for each mixture, the relatively small differences observed cannot be distinguished from experimental variability. The slight tendency towards lower AS may be related to clinker dilution and delayed hydration, which could reduce early water consumption and limit self-desiccation. Nevertheless, this interpretation remains tentative, as neither hydration kinetics nor internal relative humidity was monitored in the present study.

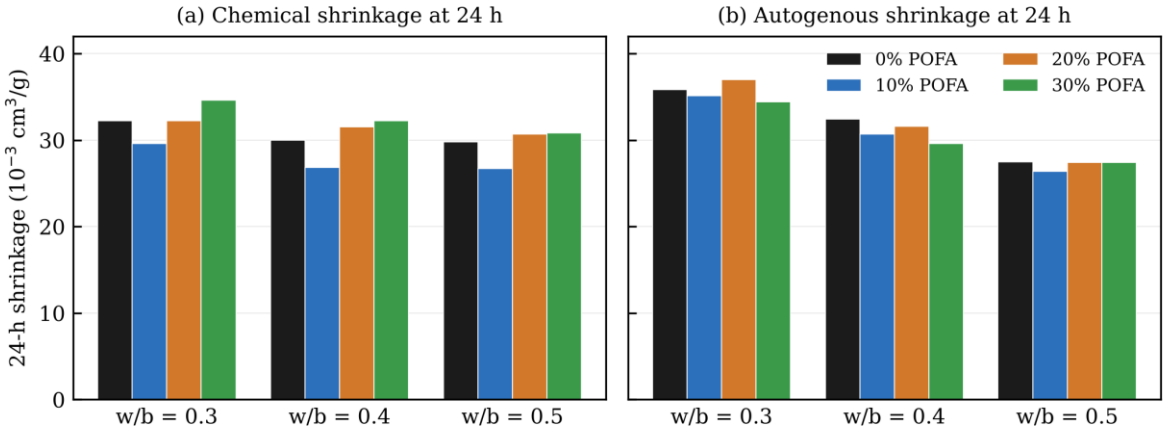


Figure 6. Effect of POFA content on (a) chemical shrinkage and (b) autogenous shrinkage at 24 h.

4.7. Relationship between chemical and autogenous shrinkage

The relationship between chemical shrinkage (CS) and autogenous shrinkage (AS) was examined using the AS/CS ratios at 24 h (Table 4). The ratios range from 0.89 to 1.19, with values exceeding unity in several mixtures, particularly at lower water-to-binder ratios. This finding is inconsistent with the expected relationship between the two phenomena after the formation of a solid skeleton, when autogenous shrinkage should not exceed chemical shrinkage [23,24]. It therefore suggests that the two measurement procedures may have introduced different experimental biases, limiting the direct comparison of the measured values.

One possible source of discrepancy is the thickness of the paste layer used in the CS test (15–24 mm). Such thickness may restrict water access to the internal pores after setting, potentially leading to an underestimation of chemical shrinkage [42]. Conversely, water penetration through the latex membrane used for AS measurements could increase the apparent submerged mass and consequently lead to an overestimation of autogenous shrinkage [43]. However, membrane watertightness and the actual contribution of these effects have not been established sufficiently to identify their respective influence. Differences in testing temperature may also have contributed to the discrepancy.

These limitations indicate that the measured AS/CS ratios should be interpreted cautiously rather than as a direct representation of the physical relationship between the two shrinkage mechanisms. Future investigations should use thinner paste layers for CS measurements, verify membrane watertightness through systematic specimen mass

checks, maintain identical temperatures for both test procedures and include replicate measurements. These improvements would provide a more reliable basis for comparing chemical and autogenous shrinkage.

5. Conclusions

This study investigated the effects of palm oil fuel ash (POFA) replacement and water-to-binder ratio on the early-age chemical shrinkage (CS) and autogenous shrinkage (AS) of cement pastes. The main objectives were to quantify the influence of the water-to-binder ratio, assess the effect of different POFA replacement levels (0%, 10%, 20% and 30%), and examine the relationship between the two shrinkage mechanisms. Chemical shrinkage was measured using the ASTM C1608-based method, while autogenous shrinkage was determined volumetrically using latex membranes and hydrostatic weighing. Both measurements were conducted over the first 24 h following water–binder contact.

The results revealed that the water-to-binder ratio affected the two shrinkage mechanisms differently. Its influence on chemical shrinkage was limited, whereas increasing the ratio from 0.3 to 0.5 reduced the 24-h autogenous shrinkage of the control paste by approximately 23%. POFA incorporation also produced different responses. The 10% replacement level consistently yielded the lowest chemical shrinkage, with reductions of approximately 8–11% compared with the corresponding control pastes. However, increasing the replacement level to 20% and 30% did not produce further reductions, and chemical shrinkage became comparable to or higher than that of the control. By contrast, the influence of POFA on autogenous shrinkage remained small, with variations ranging from −8.6% to +3.4%. These findings indicate that the reduction in chemical shrinkage observed at 10% POFA was not accompanied by a comparable change in autogenous shrinkage. They also show that the effects of supplementary cementitious materials on early-age volume changes cannot be assessed through a single shrinkage indicator.

Several limitations should be considered when interpreting these findings. Only one measurement was performed for each mixture, which prevented the evaluation of experimental variability and the application of statistical tests. In addition, the monitoring period was limited to 24 h. The comparison between CS and AS also revealed discrepancies, with AS/CS ratios ranging from 0.89 to 1.19 and exceeding unity in several mixtures. These values suggest that the two measurement procedures may not have provided fully comparable results. The relatively thick paste layers used in the chemical shrinkage test, possible water penetration through the latex membranes and differences in testing temperature may have contributed to these discrepancies; however, their respective contributions could not be established from the available measurements.

Further research should investigate the mechanisms responsible for the observed influence of POFA on early-age shrinkage by combining shrinkage measurements with isothermal calorimetry, thermogravimetric analysis and internal relative humidity monitoring. These complementary techniques would help clarify the relationships between hydration kinetics, water consumption and self-desiccation. In addition, extending the monitoring period beyond 24 h and conducting investigations on POFA-containing mortars and concretes would establish whether the trends observed in cement pastes are maintained in more complex cement-based materials and under conditions closer to practical applications. Such investigations would provide a broader understanding of the potential of POFA as a supplementary cementitious material in sustainable construction.

Appendix

A. Measured shrinkage time series

Table A1. Chemical shrinkage (10^{-3} cm^3/g of binder) versus time.

w/b	POFA (%)	0 h	3 h	6 h	9 h	12 h	15 h	18 h	21 h	24 h
0.3	0	0.0	5.4	9.2	12.6	16.6	18.9	23.8	27.6	32.2
0.3	10	0.0	5.3	8.6	11.9	14.7	17.1	21.1	24.3	29.6
0.3	20	0.0	4.8	9.2	11.8	14.6	17.1	20.8	26.1	32.2
0.3	30	0.0	6.2	10.7	13.4	16.0	18.7	23.1	30.0	34.6
0.4	0	0.0	5.2	8.5	12.0	15.4	19.2	22.7	26.3	30.0
0.4	10	0.0	5.0	8.5	10.3	13.4	16.9	21.0	24.5	26.8
0.4	20	0.0	5.3	9.5	11.9	12.7	16.9	19.7	26.1	31.5
0.4	30	0.0	5.1	10.5	13.1	15.3	18.4	22.1	28.0	32.2
0.5	0	0.0	4.7	8.7	12.3	14.6	17.5	21.2	25.3	29.8
0.5	10	0.0	3.8	7.3	10.6	13.0	16.4	19.9	23.5	26.7
0.5	20	0.0	5.3	9.4	12.0	12.6	15.7	19.4	24.8	30.7
0.5	30	0.0	5.2	9.9	13.0	14.7	17.3	21.7	26.5	30.8

Time origin (0 h): first reading, about 30 min after the first contact between water and binder.

Table A2. Autogenous shrinkage (10^{-3} cm^3/g of binder) versus time.

w/b	POFA (%)	0 h	3 h	6 h	9 h	12 h	15 h	18 h	21 h	24 h
0.3	0	0.0	6.1	10.0	14.4	18.2	22.3	26.6	30.7	35.8
0.3	10	0.0	4.2	8.8	12.2	18.2	21.0	26.5	28.8	35.1
0.3	20	0.0	6.8	10.2	15.7	19.1	24.5	26.9	32.6	37.0
0.3	30	0.0	3.6	6.7	11.8	15.9	19.8	23.5	28.2	34.4
0.4	0	0.0	4.7	7.6	12.4	15.9	21.1	23.4	28.2	32.4
0.4	10	0.0	2.3	7.9	11.3	15.5	19.9	23.8	26.1	30.7
0.4	20	0.0	3.8	9.5	13.8	15.7	21.3	25.2	28.1	31.6
0.4	30	0.0	3.9	6.1	11.0	13.7	16.7	22.4	25.3	29.6
0.5	0	0.0	1.9	5.0	9.2	11.8	17.5	19.5	23.6	27.5
0.5	10	0.0	3.7	5.3	9.8	13.8	18.4	21.3	22.5	26.4
0.5	20	0.0	3.5	8.5	10.6	15.4	18.1	21.7	25.2	27.4
0.5	30	0.0	2.5	5.7	9.3	12.3	17.1	19.2	23.4	27.4

Time origin (0 h): first reading, about 30 min after the first contact between water and binder.

CRediT authorship contribution statement

To be completed, e.g. Tubuo Fabian Mawen: Investigation, Formal analysis, Writing – original draft. Nkwenti Flavious Tanue: Conceptualization, Methodology, Supervision, Writing – review & editing. Tchemou Gilbert: Supervision. Writing – review & editing.

Declaration of competing interest

The authors declare that they have no known competing financial interests or personal relationships that could have appeared to influence the work reported in this paper. Confirm.

Funding

State any funding, or: "This research did not receive any specific grant from funding agencies in the public, commercial, or not-for-profit sectors."

Data availability

Data will be made available on request.

References

[1] J. Mitchell Crow, The concrete conundrum, Chemistry World. https://www.chemistryworld.com/features/the-concrete-conundrum/3004823.article (accessed 17 July 2018).
[2] D.P. Bentz, O.M. Jensen, Mitigation strategies for autogenous shrinkage cracking, Cem. Concr. Compos. 26 (2004) 677–685. https://doi.org/10.1016/S0958-9465(03)00045-3
[3] Md. Safiuddin, Md.A. Salam, M.Z. Jumaat, Utilization of palm oil fuel ash in concrete: a review, J. Civ. Eng. Manag. 17 (2011) 234–247. https://doi.org/10.3846/13923730.2011.574450
[4] M.Z. Al-mulali, H. Awang, H.P.S. Abdul Khalil, Z.S. Aljoumaily, The incorporation of oil palm ash in concrete as a means of recycling: a review, Cem. Concr. Compos. 55 (2015) 129–138. https://doi.org/10.1016/j.cemconcomp.2014.09.007
[5] H. Ritchie, M. Roser, Palm oil, Our World in Data (2021). https://ourworldindata.org/palm-oil (accessed 20 February 2022).
[6] K. Muthusamy, N.A. Zamri, Mechanical properties of oil palm shell lightweight aggregate concrete containing palm oil fuel ash as partial cement replacement, KSCE J. Civ. Eng. 20 (2016) 1473–1481. https://doi.org/10.1007/s12205-015-1104-7
[7] M.M.U. Islam, K.H. Mo, U.J. Alengaram, M.Z. Jumaat, Mechanical and fresh properties of sustainable oil palm shell lightweight concrete incorporating palm oil fuel ash, J. Clean. Prod. 115 (2016) 307–314. https://doi.org/10.1016/j.jclepro.2015.12.051
[8] A.M. Zeyad, M.A. Megat Johari, B.A. Tayeh, M.O. Yusuf, Pozzolanic reactivity of ultrafine palm oil fuel ash waste on strength and durability performances of high strength concrete, J. Clean. Prod. 144 (2017) 511–522. https://doi.org/10.1016/j.jclepro.2016.12.121
[9] W. Tangchirapat, T. Saeting, C. Jaturapitakkul, K. Kiattikomol, A. Siripanichgorn, Use of waste ash from palm oil industry in concrete, Waste Manag. 27 (2007) 81–88. https://doi.org/10.1016/j.wasman.2005.12.014
[10] E. Khankhaje et al., On blended cement and geopolymer concretes containing palm oil fuel ash, Mater. Des. 89 (2016) 385–398. https://doi.org/10.1016/j.matdes.2015.09.140
[11] W. Tangchirapat, C. Jaturapitakkul, Strength, drying shrinkage, and water permeability of concrete incorporating ground palm oil fuel ash, Cem. Concr. Compos. 32 (2010) 767–774. https://doi.org/10.1016/j.cemconcomp.2010.08.008
[12] J.-H. Tay, K.-Y. Show, Use of ash derived from oil-palm waste incineration as a cement replacement material, Resour. Conserv. Recycl. 13 (1995) 27–36. https://doi.org/10.1016/0921-3449(94)00012-T
[13] P. Chindaprasirt, S. Rukzon, V. Sirivivatnanon, Resistance to chloride penetration of blended Portland cement mortar containing palm oil fuel ash, rice husk ash and fly ash, Constr. Build. Mater. 22 (2008) 932–938. https://doi.org/10.1016/j.conbuildmat.2006.12.001
[14] C. Jaturapitakkul, K. Kiattikomol, W. Tangchirapat, T. Saeting, Evaluation of the sulfate resistance of concrete containing palm oil fuel ash, Constr. Build. Mater. 21 (2007) 1399–1405. https://doi.org/10.1016/j.conbuildmat.2006.07.005
[15] A.S.M. Abdul Awal, M. Warid Hussin, Effect of palm oil fuel ash in controlling heat of hydration of concrete, Procedia Eng. 14 (2011) 2650–2657. https://doi.org/10.1016/j.proeng.2011.07.333
[16] P. Chindaprasirt, S. Homwuttiwong, C. Jaturapitakkul, Strength and water permeability of concrete containing palm oil fuel ash and rice husk–bark ash, Constr. Build. Mater. 21 (2007) 1492–1499. https://doi.org/10.1016/j.conbuildmat.2006.06.015
[17] N. Ranjbar, M. Mehrali, U.J. Alengaram, H.S.C. Metselaar, M.Z. Jumaat, Compressive strength and microstructural analysis of fly ash/palm oil fuel ash based geopolymer mortar under elevated temperatures, Constr. Build. Mater. 65 (2014) 114–121. https://doi.org/10.1016/j.conbuildmat.2014.04.064
[18] S.K. Lim, C.S. Tan, O.Y. Lim, Y.L. Lee, Fresh and hardened properties of lightweight foamed concrete with palm oil fuel ash as filler, Constr. Build. Mater. 46 (2013) 39–47. https://doi.org/10.1016/j.conbuildmat.2013.04.015

[19] E. Aminudin, M.F. Md Din, M.W. Hussin, A.H. Abdullah, K. Iwao, Y. Ichikawa, Properties of agro-industrial aerated concrete as potential thermal insulation for building, MATEC Web Conf. 47 (2016) 04020. https://doi.org/10.1051/matecconf/20164704020
[20] W. Arminda, H. Awang, Replacing cement with POFA to improve the thermal properties of lightweight foamed concrete, IOP Conf. Ser. Mater. Sci. Eng. 431 (2018) 032004. https://doi.org/10.1088/1757-899X/431/3/032004
[21] S. Detphan, C. Phiangphimai, A. Wachum, S. Hanjitsuwan, T. Phoo-ngernkham, P. Chindaprasirt, Strength development and thermal conductivity of POFA lightweight geopolymer concrete incorporating FA and PC, Eng. Appl. Sci. Res. 48 (2021) 718–723.
[22] S.Y. Kong, Z.H. See, C.L. Lee, X. Yang, L.S. Wong, T.S. Goh, Thermal and mechanical properties of mortar incorporated with paraffin/palm oil fuel ash composite, J. Build. Eng. 26 (2019) 100923. https://doi.org/10.1016/j.jobe.2019.100923
[23] E.E. Holt, Early Age Autogenous Shrinkage of Concrete, VTT Publications 446, Technical Research Centre of Finland, Espoo, 2001.
[24] P. Lura, O.M. Jensen, K. van Breugel, Autogenous shrinkage in high-performance cement paste: an evaluation of basic mechanisms, Cem. Concr. Res. 33 (2003) 223–232. https://doi.org/10.1016/S0008-8846(02)00890-6
[25] S. Garcia-Boivin, Développement d'une méthode expérimentale et contribution à l'analyse physique du retrait endogène, PhD thesis, École Nationale des Ponts et Chaussées, Paris, 2001.
[26] P. Mounanga, Étude expérimentale du comportement de pâtes de ciment au très jeune âge : hydratation, retraits, propriétés thermophysiques, PhD thesis, Université de Nantes, 2004.
[27] J. Beaudoin, I. Odler, Hydration, setting and hardening of Portland cement, in: P.C. Hewlett, M. Liska (Eds.), Lea's Chemistry of Cement and Concrete, 5th ed., Butterworth-Heinemann, 2019, pp. 157–250. https://doi.org/10.1016/B978-0-08-100773-0.00005-8
[28] M. Nehdi, A.M. Soliman, Early-age properties of concrete: overview of fundamental concepts and state-of-the-art research, Proc. Inst. Civ. Eng. Constr. Mater. 164 (2011) 57–77. https://doi.org/10.1680/coma.900040
[29] O. Esping, Early age properties of self-compacting concrete – Effects of fine aggregate and limestone filler, PhD thesis, Chalmers University of Technology, Göteborg, Sweden, 2007.
[30] H. Noorvand, A.A.A. Ali, R. Demirboga, H. Noorvand, N. Farzadnia, Physical and chemical characteristics of unground palm oil fuel ash cement mortars with nanosilica, Constr. Build. Mater. 48 (2013) 1104–1113. https://doi.org/10.1016/j.conbuildmat.2013.07.070
[31] M. Vakili, M. Rafatullah, M.H. Ibrahim, B. Salamatinia, Z. Gholami, H.M. Zwain, A review on composting of oil palm biomass, Environ. Dev. Sustain. 17 (2015) 691–709. https://doi.org/10.1007/s10668-014-9581-2
[32] F. Sulaiman, N. Abdullah, H. Gerhauser, A. Shariff, An outlook of Malaysian energy, oil palm industry and its utilization of wastes as useful resources, Biomass Bioenergy 35 (2011) 3775–3786. https://doi.org/10.1016/j.biombioe.2011.06.018
[33] W. Tangchirapat, C. Jaturapitakkul, P. Chindaprasirt, Use of palm oil fuel ash as a supplementary cementitious material for producing high-strength concrete, Constr. Build. Mater. 23 (2009) 2641–2646. https://doi.org/10.1016/j.conbuildmat.2009.01.008
[34] T. Mehmannavaz, M. Ismail, S. Radin Sumadi, M.A. Rafique Bhutta, M. Samadi, S.M. Sajjadi, Binary effect of fly ash and palm oil fuel ash on heat of hydration aerated concrete, Sci. World J. 2014 (2014) 461241. https://doi.org/10.1155/2014/461241
[35] H. Awang, M.Z. Al-Mulali, The inclusion of palm oil ash biomass waste in concrete: a literature review, in: V. Waisundara (Ed.), Palm Oil, InTech, 2018. https://doi.org/10.5772/intechopen.76632
[36] K. Wi, H.-S. Lee, S. Lim, H. Song, M.W. Hussin, M.A. Ismail, Use of an agricultural by-product, nano sized palm oil fuel ash as a supplementary cementitious material, Constr. Build. Mater. 183 (2018) 139–149. https://doi.org/10.1016/j.conbuildmat.2018.06.156
[37] J.-H. Tay, Ash from oil-palm waste as a concrete material, J. Mater. Civ. Eng. 2 (1990) 94–105. https://doi.org/10.1061/(ASCE)0899-1561(1990)2:2(94)
[38] V. Sata, C. Jaturapitakkul, K. Kiattikomol, Utilization of palm oil fuel ash in high-strength concrete, J. Mater. Civ. Eng. 16 (2004) 623–628. https://doi.org/10.1061/(ASCE)0899-1561(2004)16:6(623)
[39] ASTM C618-08a, Standard Specification for Coal Fly Ash and Raw or Calcined Natural Pozzolan for Use in Concrete, ASTM International, West Conshohocken, PA, 2008.
[40] K. Abdullah, M.W. Hussin, F. Zakaria, R. Muhamad, Z.A. Hamid, POFA: a potential partial cement replacement material in aerated concrete, 2006.
[41] N.M. Altwair, M.A. Megat Johari, A.M. Zeyad, Pozzolanic characteristics of palm oil waste ash (POWA) and treated palm oil fuel ash (TPOFA), CRC Press, 2012. https://doi.org/10.1201/b13165-31
[42] ASTM C1608, Standard Test Method for Chemical Shrinkage of Hydraulic Cement Paste, ASTM International, West Conshohocken, PA.
[43] P. Lura, O.M. Jensen, Measuring techniques for autogenous strain of cement paste, Mater. Struct. 40 (2007) 431–440. https://doi.org/10.1617/s11527-006-9180-0
[44] Biyindi, T. A., Mbakop, F. K., Toumi, E., Etonleu, B. W., & Pondi, J. (2019). Comparative physico-mechanical study of cements CEM II 42.5R in Cameroon: Case of DANGOTE and CIMENCAM. Open Journal of Civil Engineering, 9(1), 18–34. https://doi.org/10.4236/ojce.2019.91002
[45] Jamo, H. U., & Abdu, S. G. (2015). Characterization of a treated palm oil fuel ash. Science World Journal, 10(1).

[46] Chindaprasirt, P., Jaturapitakkul, C., & Rattanasak, U. (2011). Effect of palm oil fuel ash fineness on the microstructure of blended cement paste. Construction and Building Materials, 25(11), 4095–4104. https://doi.org/10.1016/j.conbuildmat.2011.04.062

[47] Alsubari, B., Shafigh, P., & Jumaat, M. Z. (2015). Development of self-consolidating high strength concrete incorporating treated palm oil fuel ash. Materials, 8(5), 2154–2173. https://doi.org/10.3390/ma8052154